Russian Journal of Earth Sciences Online ISSN: 1681-1208

Integrated Geophysical Cluster Analysis for the Tectonic Zonation of the West Siberian Lithosphere

A. G. Petrunin[1,2,*], M. K. Kaban[1,3], S. Fuchs[2], and O. O. Shevaldysheva[1]

[1]Geophysical Center of the Russian Academy of Sciences (GC RAS), Moscow, Russian Federation
[2]Section Geoenergy, German Research Center for Geosciences (GFZ), Potsdam, Germany
[3]Section Earth System Modelling, German Research Center for Geosciences (GFZ), Potsdam, Germany
* **Correspondence to:** Alexey G. Petrunin, alexei@gfz.de

Abstract: We present a data-driven model for tectonic zonation of the West Siberian Basin (WSB) based on *K*-means clustering applied to a multivariate geophysical dataset. The initial analysis incorporates lithospheric thickness, crustal thickness, sedimentary thickness, topography, surface heat flow, and *S*-wave velocity anomaly at 100 km depth. F-statistics and permutation feature importance analysis indicate that only four primary parameters are sufficient to achieve reliable zonation, yielding six clusters that correspond to distinct tectonic domains. These domains reflect the complex geodynamic evolution of the region, including Paleozoic accretion, Mesozoic rifting, and subsequent subsidence. Independent data on hydrocarbon field locations demonstrate that major oil accumulations are primarily associated with two of these clusters, supporting the validity of the approach. The resulting zonation provides a reproducible basis for lithospheric regionalization and resource assessment. This framework can be further developed by integrating supervised machine learning methods to predict a specific structure and thermal regimes in areas with limited data. The quantitative characterization of these domains provides an objective framework for future geodynamic models and resource assessments.

Keywords: West Siberian Basin, cluster analysis, tectonic zonation, integrated geophysical analysis, surface heat flow, lithospheric thickness

Citation: Petrunin A. G., Kaban M. K., Fuchs S., and Shevaldysheva O. O. (2026), Integrated Geophysical Cluster Analysis for the Tectonic Zonation of the West Siberian Lithosphere, *Russian Journal of Earth Sciences*, 26, ES3001, EDN: THROIN, https://doi.org/10.2205/2026es001102

1. Introduction

The West Siberian Basin (WSB) is one of the largest intracratonic sedimentary basins globally, spanning approximately 2.6 million km^2 and serving as a major hydrocarbon province with proven reserves exceeding 146 billion barrels of oil and 45 trillion cubic meters of gas [*Khafizov et al.*, 2022; *Ulmishek*, 2003; *Verma and Ulmishek*, 2003]. Due to its economic importance, the WSB region is densely covered by both geological and geophysical surveys.

The WSB is bordered by the Ural Mountains to the west, the Yenisey River to the east, and the Altai-Sayan fold belts to the south [*Artyushkov and Chekhovich*, 2023; *Vetrov et al.*, 2021]. It evolved as an undeformed Mesozoic sag overlying a heterogeneous Hercynian accreted terrane and an Early Triassic rift system [*Latyshev et al.*, 2025; *Pavlov*, 1995; *Vibe et al.*, 2018]. The basement comprises foldbelts deformed during the Late Carboniferous–Permian collision of the Siberian, Kazakhstan, and Russian cratons, resulting in a mosaic of relict ocean basins, microcontinents, and extinct arc systems [*Ivanov*, 2007; *Saunders et al.*, 2005]. This incomplete collision was followed by Early Mesozoic rifting, linked to Permian–Triassic Siberian Trap volcanism, which established the basin's structural framework [*Burgess and Black*, 2025; *Latyshev et al.*, 2025]. Subsequent passive subsidence from the Jurassic to Oligocene accumulated a thick sedimentary cover of Middle Triassic through Tertiary clastic rocks, reaching 8–10 km in graben-like zones [*Artyushkov and Chekhovich*, 2023; *Khafizov et al.*, 2022].

Research Article

Received: November 12, 2025
Accepted: February 5, 2026
Published: June 22, 2026

Geophysical studies reveal a heterogeneous lithosphere in the WSB, distinct from the ancient Siberian Platform. Lithospheric thickness averages 130 km, ranging from 65 km in the south to 200 km in its central part [*Cherepanova et al.*, 2013; *Pasyanos et al.*, 2014]. Crustal thickness varies from 30 to 55 km, with the thinnest sections (30–33 km) underlying thick Mesozoic deposits and slightly thicker crust (36–39 km) in rift zones, contrasting with the 45–50 km crust of ancient shields [*Laske et al.*, 2013; *Mooney et al.*, 2023]. The sedimentary cover, primarily clastic, correlates with basement depth, achieving maximum thicknesses in northern regions where the crystalline basement lies at 8–10 km [*Ulmishek*, 2003; *Vibe et al.*, 2018].

Surface heat flow averages 55–65 mW/m^2, reaching 70–80 mW/m^2 in rift basins and fault zones, which is attributed to mantle heat sources [*Brown et al.*, 2003]. Another parameter, which is usually considered as a proxy for the thermal state of the lithosphere, is *S*-wave velocity anomalies, which inversely correlate with temperature: positive (relatively higher seismic velocities) anomalies as a rule indicate a cold, stable lithosphere, while negative ones suggest warmer, thinner lithosphere, more tectonically active regions [*Kaban et al.*, 2016; *Shapiro and Ritzwoller*, 2004]. Modern high-resolution tomographic models, such as SL2013sv and REVEAL, effectively resolve upper-mantle details at depths of 100–250 km [*Schaeffer and Lebedev*, 2013; *Thrastarson et al.*, 2024], enabling their use in regional studies, where resolution in both vertical and lateral directions is essential.

Traditional tectonic zonation is typically based on qualitative interpretation of geological maps, tectonic features, or individual geophysical parameters. However, such approaches often do not adequately reflect the complexity of lithospheric structure, as shown in previous studies. In particular, analyses that rely on a single parameter, for example, crustal thickness, seismic velocity, or heat flow, can result in ambiguous or even conflicting interpretations. For example, a high-velocity anomaly may indicate a cold and rigid lithosphere in a stable continental region, whereas the same feature can also be associated with a domain of different composition, such as a mafic underplate or the presence of eclogite. As a result, this non-uniqueness poses a significant challenge for geophysical inversion, since seismic data alone are insufficient to distinguish between temperature variations and chemical heterogeneity with high confidence. Therefore, the modern approach to interpreting geological and geophysical data is based on a more comprehensive analysis that considers multiple parameters and their interrelationships.

Cluster analysis has previously been applied to lithospheric zonation using diverse geophysical, geological, and geodynamic datasets for various purposes, such as regional tectonic and geodynamic interpretation [*Nikolaev*, 2005; *Sokolov and Mazarovich*, 2016]. For lithospheric-scale zonation, which accounts for the most significant features such as crustal, sedimentary, and lithospheric thicknesses, as well as proxy indicators of the thermal structure, we propose an approach based on an integrated multi-parameter analysis. This method enables the objective classification of lithospheric domains by applying unsupervised statistical techniques, such as *K*-means clustering, to delineate domains based on their structural and physical properties.

To demonstrate the application of the clustering algorithm to a multi-parameter geophysical dataset for the West Siberian lithosphere, we consider six parameters: lithospheric thickness (H_l), crustal thickness (H_c), sedimentary layer thickness (H_s), surface heat flow (Q), topography, and *S*-wave velocity anomaly at 100 km depth (dV_s_100). We then assess the influence and significance of each parameter on the clustering results. The main objective is to enhance the methodology for tectonic zoning based on statistical analysis of lithospheric structure and geophysical data. The workflow includes determining the optimal number of clusters, evaluating their statistical characteristics, and providing an interpretation by comparing the resulting clusters with known geological features and typical structural characteristics for different types of the continental lithosphere.

2. Data and Methodology

To investigate the tectonic zonation of the West Siberian lithosphere, we compiled a dataset of geophysical parameters. Namely, we focused on six key parameters: lithospheric thickness (H_l), crustal thickness (H_c), sedimentary layer thickness (H_s), surface heat flow (Q), topography (topo), and S-wave velocity anomaly at 100 km (dV_s_100). These parameters were selected to provide a comprehensive representation of the lithosphere's physical properties, thermal state, and structural variations, which are essential for understanding the tectonic framework and evolution of the West Siberian Basin.

Lithospheric thickness reflects the overall rigidity and thermal structure of the lithospheric plate. This parameter is critical for identifying variations in lithospheric strength influenced by past tectonic processes, such as rifting or plume activity, as supported by global thermal models [*Artemieva*, 2006].

Crustal thickness, derived from seismic models such as CRUST1.0 [*Laske et al.*, 2013] or ECM1 [*Mooney et al.*, 2023], reveals differences in crustal composition and tectonic history, helping to distinguish between stable cratonic regions and tectonically active zones, particularly in areas with evidence of ancient rift structures [*Pavlov*, 1995].

The thickness of the sedimentary layer serves as a key indicator of basin formation and subsidence history. In the West Siberian Basin, thick sedimentary sequences are linked to tectonic evolution, reflecting a complex mechanism of the sedimentary subsidence involving interplay between post-rift cooling of the lithosphere, prograde metamorphism [*Artyushkov and Chekhovich*, 2023], mantle plume impacts [*Holt et al.*, 2012], and dynamic topography [*Vibe et al.*, 2018].

Surface heat flow, compiled from databases like the IHFC Global Heat Flow Database [*Duchkov et al.*, 2012; *Fuchs et al.*, 2023; *Haeger et al.*, 2022; *Neumann et al.*, 2025], provides insights into the thermal regime of the lithosphere. Lateral variations in heat flow reflect variations in crustal composition, lithospheric structure, mantle dynamics, and prior tectonic activity, such as volcanism associated with the Siberian Traps [*Latyshev et al.*, 2025; *Reichow et al.*, 2009].

Topography reflects the surface expression of tectonic processes, isostatic adjustments, and dynamic topography, which in the West Siberian Basin are influenced by subsidence and mantle dynamics [*Saunders et al.*, 2005; *Vibe et al.*, 2018]. Although the topography at the WSB is low, ranging from 0 to 600 m, it may also be a valuable parameter for identifying different clusters of the lithospheric structure.

Finally, the S-wave velocity anomaly at 100 km, derived from seismic tomography models [*Schaeffer and Lebedev*, 2013; *Thrastarson et al.*, 2024], indicates variations in mantle composition, temperature, and viscosity within the lithospheric mantle. This parameter is sensitive to mantle dynamics, such as plume-related anomalies or lithospheric thinning, complementing the other parameters by providing deeper structural insights. A depth of 100 km is chosen as a proxy for the lithospheric mantle thermal state, with minimal influence from crustal-scale subsurface factors.

Although other geophysical parameters, such as gravity and magnetic fields, provide valuable insights into the subsurface structure, they were not included in this analysis.

We decided to exclude these parameters, considering the principles of cluster analysis, which emphasize minimizing the number of input parameters to reduce dimensionality and avoid or minimize the use of directly correlated parameters [*Guyon and Elisseeff*, 2003; *Koller and Sahami*, 1996; *Witten and Tibshirani*, 2010]. For instance, while gravity data may correlate strongly with crustal and lithospheric thickness [*Kaban et al.*, 2016], magnetic anomalies often reflect upper-crustal composition but may not provide unique information beyond what is already provided by seismic and thermal parameters.

Thus, the chosen parameters (H_l, H_c, H_s, Q, topo, dV_s_100) are relatively independent, capturing distinct aspects of lithospheric properties without significant overlap. Moreover, we will further study the influence of each parameter on cluster recognition by applying both F-statistics and permutation feature importance methods to maximize dimensionality reduction in the input data vector without significantly affecting the final result.

2.1. Data Sources and Compilation

To ensure reproducibility and consistency, we utilized data from publicly available global and regional geophysical models. The input datasets have different original resolutions and grids, not necessarily aligned with each other. To harmonize these datasets, we mapped all parameters onto a uniform $0.5° \times 0.5°$ spatial grid, providing the sufficient resolution required to capture regional features. Data from models with varying resolutions were regridded using ordinary Kriging [*Stein*, 1999] on a sphere, implemented in Python's `PyKrige` package, to ensure spatial continuity and consistency across the study area [*Murphy*, 2014]. This approach provides spatial continuity and ensures that the resulting dataset is internally consistent across the entire study area. The parameters included in the analysis, along with their respective units, sources, and value range, are summarized in Table 1. Note that the layer thickness is defined as the difference between the depths of the base and the top of the corresponding layer.

Table 1. Summary of geophysical parameters used in the study

Parameter	Symbol	Unit	Data source	Value range
Lithospheric Thickness	H_l	km	LITHO1.0 model [*Pasyanos et al.*, 2014]	~65 to 200 km
Crustal Thickness	H_c	km	CRUST1.0 model [*Laske et al.*, 2013]	~30 to 50 km
Sedimentary Layer Thickness	H_s	km	Derived from CRUST1.0 basement depth	Up to 8–12 km
Surface Heat Flow	Q	mW/m^2	IHFC database [*Duchkov et al.*, 2012; *Fuchs et al.*, 2023; *Neumann et al.*, 2025]	25 to 80 mW/m^2
S-wave Velocity Anomaly	dV_s_100	km/s	REVEAL model [*Thrastarson et al.*, 2024]	–0.2 to +0.2 km/s
Topography	topo	m	[*Tozer et al.*, 2019]	0–450 m

The lithospheric structure in this study is constrained using the CRUST1.0 [*Laske et al.*, 2013] and LITHO1.0 [*Pasyanos et al.*, 2014] models. Sedimentary thickness (H_s) is determined by subtracting the depth to the crystalline basement, as defined by CRUST1.0, from the surface elevation [*Tozer et al.*, 2019]. The S-wave velocity anomaly at a depth of 100 km (dV_s_100) is taken from the REVEAL model [*Thrastarson et al.*, 2024], which provides high spatial resolution for the Eurasian continent at this depth, with dV_s_100 values ranging from –0.2 to +0.2 km/s. All parameters are integrated into a unified dataset, where each geographic location is characterized by a vector of co-located values. This approach provides the basis for the subsequent clustering analysis.

Lithospheric thickness (H_l), as defined by the LITHO1.0 model [*Pasyanos et al.*, 2014], varies from approximately 65 km in regions affected by rifting or plume activity to 200 km in stable cratonic areas [*Artemieva and Mooney*, 2001]. Crustal thickness (H_c) based on CRUST1.0 [*Laske et al.*, 2013] ranges from 30 to 50 km, with the thinnest crust observed in the central WSB, suggesting limited crustal stretching [*Artyushkov and Chekhovich*, 2023]. Sedimentary layer thickness (H_s), calculated as the difference between surface elevation and crystalline basement depth, reaches 8–12 km in the main depocenters [*Vyssotski et al.*, 2006]. Surface heat flow (Q), derived from the IHFC Global Heat Flow Database and Geothermal Atlas of Siberia and the Far East [*Duchkov et al.*, 2012; *Fuchs et al.*, 2023; *Neumann et al.*, 2025], ranges from maxima 80 mW/m^2 associated with the crustal structures of the Ural Foldbelt in the west and central basin highs, to sharp minima (<25 mW/m^2) along the Yenisey-Khatanga Basin in the northeast, which reflects the influence of the cold, stable lithosphere of the adjacent Siberian Craton on the basin's overall thermal regime [*Dorofeeva and Duchkov*, 2022]. The S-wave velocity anomaly at a depth of 100 km (dV_s_100) from the REVEAL model [*Thrastarson et al.*, 2024] spans a range of –0.2 to +0.2 km/s, revealing a distinct contrast between the surrounding foldbelts, which reflects lithospheric heterogeneity due to thermal or compositional variations. The most significant high-

velocity anomaly ($dV_s\_100 > 0.17$) is located along the western margin of the basin near the Ural Foldbelt, reflecting a deep, cold, and stable lithospheric root formed during the late Paleozoic Uralian Orogeny. In contrast, the lowest velocity anomaly ($dV_s\_100 < -0.07$ km/s) is found beneath the Altai-Sayan Foldbelts in the southeast, indicating a hotter, thinner, and mechanically weaker lithosphere that is more prone to far-field Cenozoic tectonic reactivation and mantle flow associated with the India-Eurasia collision. Topography, according to [*Tozer et al.*, 2019], is low, ranging from 0 to 500 m, consistent with the WSB's classification as a lowland basin influenced by dynamic topography [*Vibe et al.*, 2018] and ongoing erosional processes.

Figure 1 presents the spatial distribution of the key geophysical parameters, illustrating the structural and thermal variability across the WSB. All parameters are integrated into a unified dataset, with each location represented by a vector of co-located values, providing the basis for clustering analysis to delineate distinct geophysical domains within the WSB.

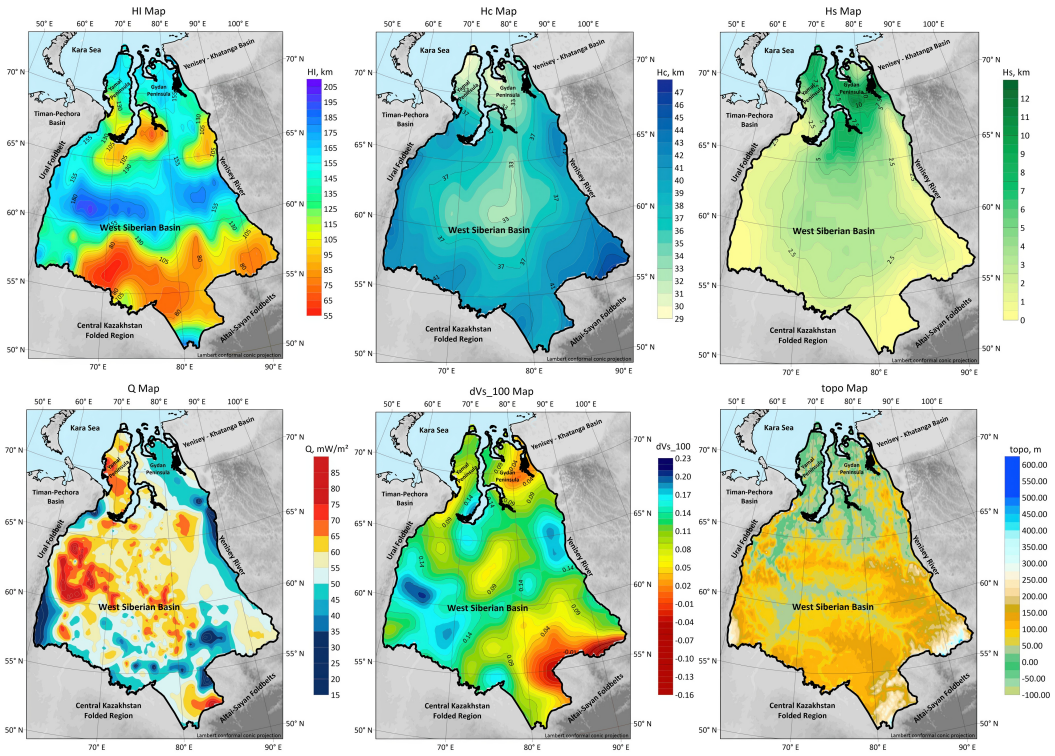

Figure 1. Spatial distribution of lithospheric (H_l), crustal (H_c), sedimentary (H_s) thickness across West Siberian Lowland (WSL), derived from the LITHO1.0 and CRUST 1.0 models [*Laske et al.*, 2013; *Pasyanos et al.*, 2014], heat flow (Q) [*Duchkov et al.*, 2012; *Fuchs et al.*, 2023; *Neumann et al.*, 2025], S-wave velocity anomaly at a depth of 100 km (dV_s_100) [*Thrastarson et al.*, 2024], and topography (topo) [*Tozer et al.*, 2019].

2.2. Methods

To investigate the tectonic zonation of the West Siberian lithosphere, we use an integrated workflow that combines geophysical data processing with advanced statistical analysis. The methodology comprises four principal stages. First, we normalize the input data to ensure that all parameters contribute equally to the analysis. Second, we select the most significant variables, thereby reducing noise and focusing on those parameters that most strongly influence the results. Third, we apply Principal Component Analysis (PCA) to reduce the dataset's dimensionality (if necessary) and identify the principal sources of variation within the data. Finally, we use K-means clustering to partition the study area into geophysically distinct tectonic domains. This sequence of steps enables a systematic

reduction of data complexity, facilitating the identification of robust tectonic patterns, as demonstrated in previous studies [*Jolliffe and Cadima*, 2016; *Pedregosa et al.*, 2012].

The geophysical parameters we use vary in scale and units (e.g., H_l ranging over 90 km versus dV_s_100 varying by less than ±0.2 km/s). Without normalization, parameters with larger ranges could disproportionately influence clustering, overshadowing smaller-scale variables [*Pedregosa et al.*, 2012]. To address this, we applied Z-score scaling, standardizing each parameter to a mean of zero and a standard deviation of one. This transformation ensured that all parameters contributed equally to the *K*-means clustering algorithm, enhancing the fairness and accuracy of the tectonic zonation.

2.3. Parameter Selection

To optimize clustering performance, we evaluated the importance of all six initial geophysical parameters (H_l, H_c, H_s, Q, topo, and dV_s_100). We used two methods to assess their significance: the F-statistic from Analysis of Variance (ANOVA) and permutation feature importance from a Random Forest Classifier [*Breiman*, 2001; *Field*, 2024]. The F-statistic (ANOVA) test evaluates whether the means of a parameter differ significantly across clusters. A high F-statistic indicates that a parameter effectively distinguishes clusters. The Permutation feature importance technique measures the contribution of each parameter to the predictive accuracy of a Random Forest Classifier trained to predict cluster assignments. Thus, the complementary usage of these methods provides more detailed information on the importance of each parameter.

The result of our analysis (Figure 2) showed that Q, topo, and dV_s_100 had the lowest F-values (around 2000), suggesting their limited ability to discriminate between clusters. Further, we performed a permutation test by shuffling parameter values and quantifying the resulting decrease in model accuracy.

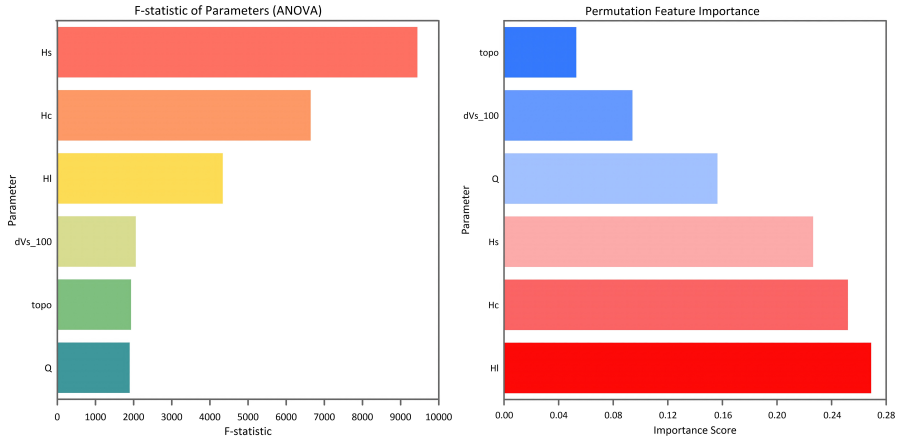

Figure 2. F-statistics (*left*) and permutation feature importance (*right*) for six parameters.

This approach revealed that parameters topo and dV_s_100 yield the lowest importance scores, approximately 0.05 and 0.1, respectively, and therefore demonstrate minimal influence on the differentiation of clusters (Figure 2). Based on these results, we excluded topo and dV_s_100 from further consideration due to their low importance scores and limited contribution to cluster separation. The exclusion of these two parameters can be explained on physical grounds. The variation of V_s within the lithosphere primarily reflects its temperature state (and composition to some extent), which is already accounted for in heat flow density (Q). The topography in the WSB is low (<450 m) and significantly influenced by erosion, resulting in a "noisy" dataset with weak discriminatory power. Thus, the final dataset includes four primary parameters (H_l, H_c, H_s, and Q), which were retained for further analysis.

The reduced dataset shows significantly higher significance for each parameter (Figure 3), suggesting that the selected dataset is a minimally valuable set that captures the heterogeneity of the lithospheric structure.

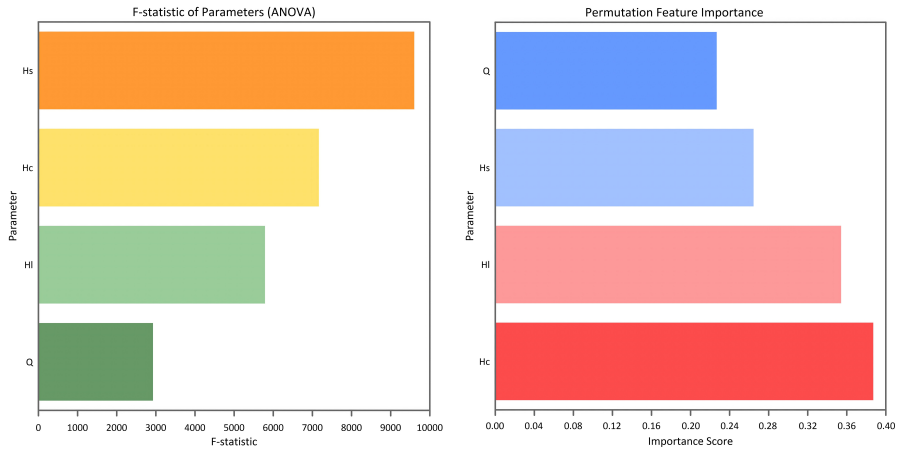

Figure 3. F-statistics (*left*) and permutation feature importance (*right*) for the final set of four parameters.

It is worth noting that we use widely adopted, publicly available global models, CRUST1.0 and LITHO1.0 [*Laske et al.*, 2013; *Pasyanos et al.*, 2014], at a standard $1° \times 1°$ resolution to ensure reproducibility. However, we assume that overlaying multiple datasets improves the effective resolution for clustering. Additionally, we include surface heat flow data, which has a higher resolution despite its limited significance in the analysis (Figure 3). Future studies might validate this approach using regional models with finer resolution to improve the tectonic zonation.

2.4. Principal Component Analysis (PCA)

We applied PCA to transform the four selected parameters into a set of uncorrelated principal components, capturing the dataset's primary variations [*Jolliffe and Cadima*, 2016]. This method helps uncover which parameters drive differences across the region, making clustering more effective. It also simplifies complex data and reveals underlying tectonic patterns in the West Siberian lithosphere. According to the PCA explained variance analysis, the first three components already account for approximately 54%, 78%, and 97% of the data variance, respectively. Figure 4 demonstrates the influence of each parameter in the principal components space. The PC1, primarily driven by positive H_c (0.64) and negative H_s (–0.53) and H_l (–0.46) loadings, distinguishes regions with thick crust and thin sedimentary cover, indicative of stable platforms. PC2, dominated by Q (0.76) and negative H_s (–0.54), highlights thermally active zones with thin sedimentary layers. PC3, led by H_l (0.77) and negative Q (–0.55), identifies stable cratonic regions with thick lithosphere. PC4, influenced by H_c (0.75) and H_s (0.58), reflects sedimentary basins with thick crust.

2.5. K-means Clustering

For the clustering procedure, we selected K-means clustering for its computational efficiency and ability to identify distinct boundaries in large datasets. This algorithm partitions data into a predefined number of clusters (k) by minimizing the within-cluster sum of squares (WCSS), a measure of intra-cluster variance [*Hartigan and Wong*, 1979]. The process involves iteratively assigning each data point to the nearest centroid based on the Euclidean distance and updating the centroids as the mean of the assigned points.

For robust tectonic zonation, determining the optimal number of clusters (k) is important. We employed three complementary methods to ensure a reliable choice. First, the elbow method involved plotting WCSS against k-values ranging from 1 to 12, identifying the point at which the WCSS reduction rate slowed, indicating a k-value between 6 and 8, and suggesting a limited benefit from additional clusters [*Mirkin*, 2011]. Second, the silhouette method calculated the average silhouette score, which quantifies how well each point fits within its cluster relative to others, with higher scores indicating better-defined

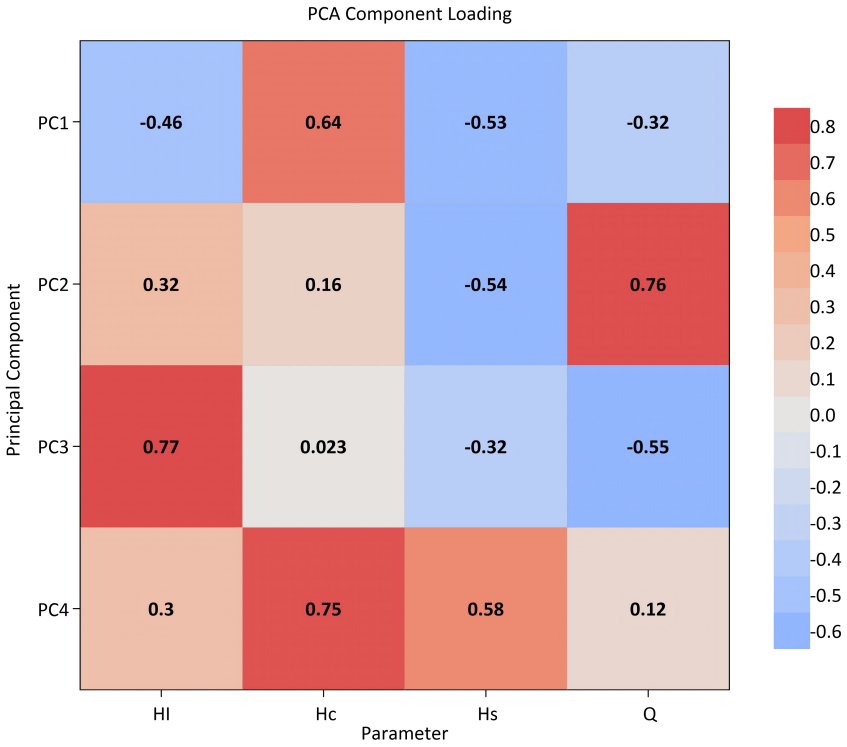

Figure 4. Heatmap of PCA component loadings, illustrating how each parameter (H_l, H_c, H_s, Q) contributes to the principal components. Brighter colors indicate stronger relationships. The digits in the cells represent the PCA component loading values for each parameter.

clusters [*Rousseeuw*, 1987]. The maximum score was observed at $k = 8$. Third, the Caliński-Harabasz index evaluated cluster quality by comparing between-cluster to within-cluster dispersion, with the highest score at $k = 4$, confirming well-separated clusters [*Calinski and Harabasz*, 1974; *Hubert and Arabie*, 1985]. Since there is an insignificant difference in the k-value suggested by these three methods, we choose $k = 6$ as a compromise solution for the optimal number of clusters.

The K-means clustering procedure was implemented using Python's scikit-learn library [*Pedregosa et al.*, 2012]. Geophysical parameters were standardized to ensure equal weighting. Principal component analysis (PCA) was applied to reduce dimensionality while preserving key variance [*Jolliffe and Cadima*, 2016]. Clustering was performed with $k = 6$, and the resulting assignments were spatially mapped to visualize tectonic domains across the West Siberian Basin (Figure 5).

To confirm the stability of the cluster determination, we conducted several validation steps. A one-way ANOVA revealed significant differences in parameter means across clusters (all $p < 0.001$), indicating distinct tectonic signatures [*Field*, 2024]. A Random Forest classifier, trained on the geophysical parameters, achieved 99% accuracy in predicting cluster membership, with permutation-based feature importance highlighting H_c (0.39), H_l (0.35), H_s (0.27), and Q (0.23) as key contributors [*Breiman*, 2001]. Cluster stability was assessed using the Adjusted Rand Index (ARI) over 100 runs, yielding a mean ARI of 0.9975 for `k-means++' initialization and 0.9965 for random initialization, demonstrating high consistency [*Hubert and Arabie*, 1985].

3. Results

After preliminary data preparation, we applied K-means clustering to an integrated geophysical dataset of the West Siberian lithosphere, revealing distinct spatial zoning. Each cluster forms a relatively coherent, contiguous region on the map, supporting the validity of the clustering. It suggests the domains reflect a specific set of lithospheric structure parameters (Figure 5).

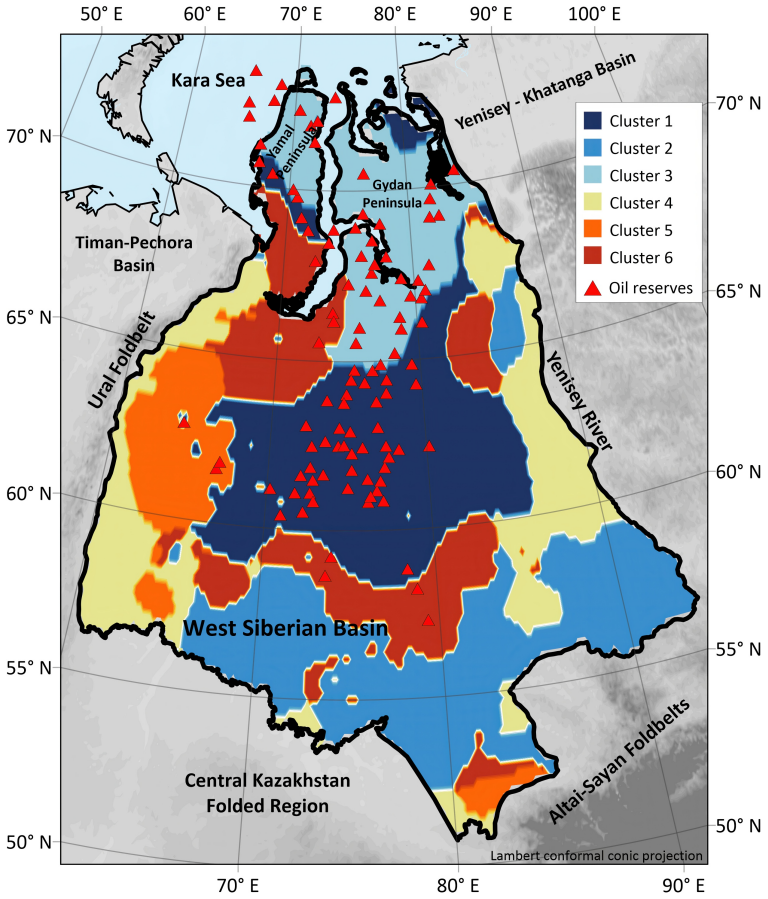

Figure 5. Spatial distribution of the six clusters across the West Siberian Basin (bounded by the thick black line). Each cluster is color-coded, presenting distinct domains derived from the integrated geophysical dataset. Red triangles represent locations of hydrocarbon giant fields within the WSB [*Khafizov et al.*, 2022].

Cluster 1 is primarily located in the central and northern parts of the West Siberian Basin, including also parts of the Yamal and Gydan Peninsulas. It is surrounded by cluster 6 (from south, north-west, and north-east), cluster 5 from the west, and cluster 3 from the north. Cluster 4 is mostly located along the Ural Foldbelt in the west and the Yenisey River in the east of the WSB, and seems to characterize the modified lithosphere between the basin margin and surrounding folding regions. Cluster 2 occupies mostly the southern margin of the WSB along the Central Kazakhstan and Altay-Sayan Foldbelts.

The observed patchy structures in some clusters, such as inclusions of Cluster 6 within Cluster 2 or Cluster 1 within Cluster 5 (Figure 5), may reflect the inherent geological heterogeneity of transitional zones, as also evidenced by oil reserves near the Cluster 1 patches. These areas often mark boundaries between tectonic domains, where lithospheric properties vary sharply due to Paleozoic accretion, Mesozoic rifting, and faulting [*Saunders et al.*, 2005; *Vyssotski et al.*, 2006]. However, some patchiness may arise from data resolution limits, as the global models have nominal $1° \times 1°$ grids, potentially introducing some artifacts at the $0.5° \times 0.5°$ clustering scale.

A significant observation is the strong spatial correlation between the locations of hydrocarbon giant fields (red triangles in Figure 5) and clusters 1 and 3. The majority of the marked oil and gas reserves are located almost entirely within the boundaries of these clusters, indicating that the lithospheric and heat flow characteristics defined by these specific clusters are potentially indicative of a favorable geodynamic environment for hydrocarbon accumulation in the WSB.

In Figure 6, we summarized mean values for four key geophysical parameters in each cluster: lithospheric thickness (H_l), crustal thickness (H_c), sedimentary layer thickness (H_s), and surface heat flow (Q).

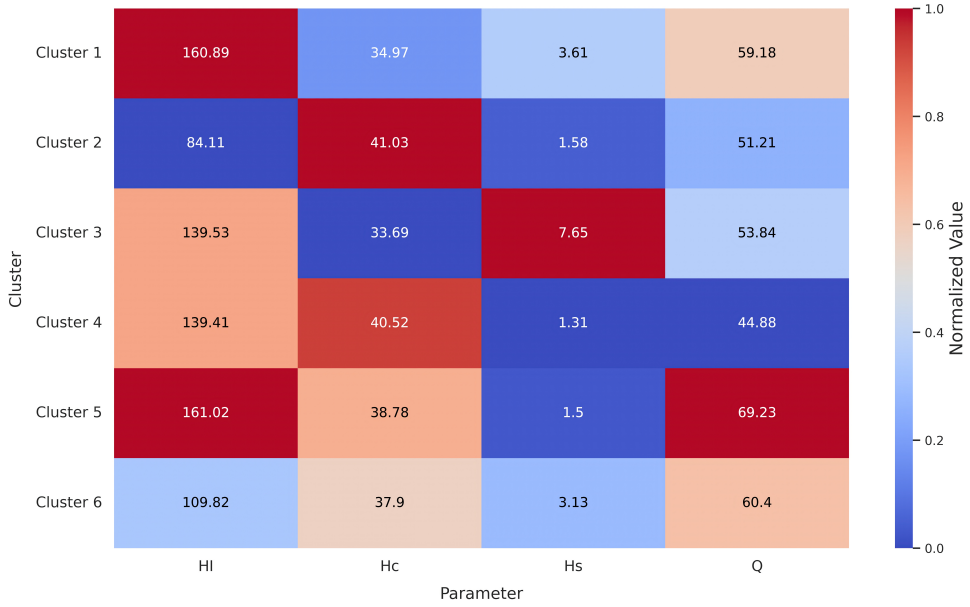

Figure 6. Heatmap plot visualizing mean values of parameters for each cluster (digits in cells) and its relative normalized magnitude (colors). Brighter colors indicate maximum (minimum) normalized value.

Colors indicating the normalized magnitude for each parameter, together with the mean values in cells, provide an explicit visualization that reveals distinct cluster signatures and are convenient for further interpretation. For instance, cluster 1 shows high H_l (160.89 km) and moderate Q (59.18 mW/m^2). Cluster 5 has both the highest H_l (161.02 km) and the highest heat flow (69.23 mW/m^2). Cluster 3 features the thickest sediment cover (7.65 km) but relatively low crustal thickness (33.69 km). These clear patterns form a unique signature for each cluster we will discuss in detail in the next section.

4. Discussion

The K-means clustering with six groups reveals distinct geodynamic domains in the West Siberian Basin. We base this on mean values of lithospheric thickness (H_l), crustal thickness (H_c), sedimentary thickness (H_s), and surface heat flow (Q). Each cluster aligns with key tectonic features summarized in Figure 6. We interpret them below.

Cluster 1 is characterized by a thick lithosphere with moderate heat flow. It dominates the central and north-central West Siberian Basin, forming large contiguous areas with many hydrocarbon reserves. This cluster has one of the thickest lithospheres (mean H_l = 161 km), suggesting stable cratonic roots, possibly from Precambrian stabilization. Moderate heat flow (Q = 59 mW/m^2 on average) correlates with relatively thin crust (H_c = 35 km) and a thin sedimentary cover (H_s = 4 km), which aligns with rift structures [*Cherepanova et al.*, 2013; *Pavlov*, 1995]. Oil and gas reserves are mainly linked to preserved Triassic rift traps [*Peterson and Clarke*, 1991; *Vyssotski et al.*, 2006].

Cluster 2 demonstrates several extreme features, including the thinnest lithosphere and the thickest crustal layer. It occupies southern regions, neighboring the Central Kazakhstan folded region and the Altai-Sayan foldbelt system. Thin lithosphere (mean H_l = 84 km) points to extension and thinning from the Paleozoic orogeny. The mean crustal thickness is larger across all clusters (H_c = 41 km) and may reflect a folded basement. Relatively low heat flow (Q = 51 mW/m^2) may suggest post-orogenic cooling [*Artemieva and Mooney*, 2001; *Şengör et al.*, 1993; *Vetrov et al.*, 2021]. This cluster represents transitional

crust influenced by Altaid tectonics (Caledonian orogeny). The disruption of Cluster 2 continuity by inclusions characterized as clusters 4 and 6 between longitudes 72°E and 77°E can be explained by the fact that this area lies within the Hercynian orogeny, which crosses more ancient Caledonian orogeny formations.

The next cluster (Cluster 3) demonstrates the thickest sediment cover (mean H_s = 7.7 km) and thinnest crust (H_c = 33.7 km on average). This cluster appears in the northern and northeastern parts of the WSB, including the edges of the Yamal and Gydan Peninsulas. The combination of thick sediments and thin crust may indicate prolonged subsidence without strong stretching and can be attributed to mantle-driven dynamic topography [*Artyushkov and Chekhovich*, 2023; *Holt et al.*, 2012; *Vibe et al.*, 2018]. With moderate heat flow and lithospheric thickness (Q = 54 mW/m^2, H_l = 140 km), this cluster, like Cluster 1, shows a high concentration of the oil and gas fields.

Cluster 4 embraces the WSB from the west, along the Ural Foldbelt, and from the southeast, along the Yenisey River, and also forms scattered southern patches. A relatively stable lithosphere (mean H_l = 140 km) and a relatively thick crust (H_c = 40.5 km) suggest collisional remnants at the boundary between the WSB and surrounding orogens. The lowest heat flow (Q = 45 mW/m^2) and sedimentary thickness (H_s = 1.3 km on average) among other clusters implies minimal recent tectonic activity [*Braitenberg and Ebbing*, 2009; *Brown et al.*, 2003; *Kaban et al.*, 2016]. It is worth noting that the western and eastern parts of the cluster belong to different episodes of tectonic history. The western segment corresponds to the Uralides, while the other segment represents the Neoproterozoic Baikalides, which frame the eastern boundary of the Siberian Platform. Although these segments originated at different times, they exhibit similar tectonic characteristics. Both overlie ancient orogenic basements: Paleozoic ophiolitic and granitic-gneissic complexes in the Uralides, and Neoproterozoic accreted terranes with ophiolitic fragments in the Baikalides. These regions are dominated by low-radioactivity lithologies (0.2–1.5 μW/m^3) and lack evidence of Mesozoic rift-related lithospheric thinning or mantle heat input [*Brown et al.*, 2003; *Gordienko*, 2006; *Puchkov*, 1997]. This is a cold, rigid, and thermally equilibrated lithosphere with low radioactivity crust, which may explain the low heat flow.

Cluster 5 is characterized by the maximum thickness of the lithosphere (H_l = 161 km), comparable to the lithosphere typical of Cluster 1, to which it adjoins from the west. However, unlike Cluster 1, it is characterized by the thinnest sedimentary layer (H_s = 1.5 km) and the highest heat flow (Q = 69 mW/m^2). Cluster 5 also lies within the Uralian Hercynides complex as the western part of Cluster 4. These two clusters have similar parameters except for heat flow (the smallest and largest among the other clusters, respectively). We can attribute it to a combination of enhanced radiogenic heat production in U-enriched granitic rocks of the adjacent Ural Foldbelt, contributing ca. 15–25 mW/m^2, latent heat release from buried Permian–Triassic silicic intrusions linked to the Siberian Traps large igneous province [*Latyshev et al.*, 2025; *Reichow et al.*, 2009; *Saunders et al.*, 2005], and probably minor edge-driven mantle convection at the lithosphere thickness step along the Ural front that can add ca. 10 mW/m^2 without bulk thinning [*Holt et al.*, 2012]. This integrated mechanism preserves lithospheric stability while elevating heat flow, consistent with the region's tectonic history.

Cluster 6 exhibits moderate parameters (H_l = 110 km, H_c = 38 km, H_s = 3 km, Q = 61 mW/m^2) and forms three major patches that embrace Cluster 1 from the south, northwest, and northeast. This spatial distribution may define Cluster 6 as a transitional domain between the thick-lithosphere core of the central WSB (Cluster 1) and the thinner, more deformed margins (Clusters 2). The northwestern segment of the cluster marks the transition to Cluster 4, which is similar to Cluster 3 in terms of lithospheric thickness. The intermediate values reflect partial lithospheric thinning, mild subsidence, and balanced heat flow driven by Triassic rifting superimposed on Permian–Triassic plume modification, creating hydrocarbon-prone traps without extreme sediment loading or thermal anomalies [*Clarke*, 1994; *Ivanov*, 2007; *Khafizov et al.*, 2022]. Thus, Cluster 6 can be determined as a transition from the central part of the WSB to its margins.

The identified clusters integrate multiple geophysical parameters, which reduces ambiguities in individual interpretations. For instance, it clarifies the causes of seismic velocity anomalies, such as thermal versus compositional effects [*Kaban et al.*, 2016; *Priestley and McKenzie*, 2013]. For example, Cluster 4, which has already been considered, aligns with a cold, stable domain, which allows for more confident attribution of positive *S*-wave anomalies to low temperatures rather than to composition alone [*Schaeffer and Lebedev*, 2013; *Shapiro and Ritzwoller*, 2004].

Thus, these clusters highlight the basin's heterogeneous geodynamics, driven by rifting, plumes, and orogeny. For clarity, we ignored minor parameter variations within clusters.

5. Conclusion

In this study, we applied the *K*-means clustering to a multivariate geophysical dataset to achieve tectonic zonation of the West Siberian Basin (WSB). The initial dataset comprises lithospheric thickness (H_l), crustal thickness (H_c), sedimentary layer thickness (H_s), surface heat flow (Q), topography, and *S*-wave velocity anomaly at 100 km depth (dV_s_100). Prior to clustering, all variables were normalized to ensure comparability and the importance of each component of the primary datasets. It allowed us to select the components critical for the determination of distinct clusters.

The clustering results delineate distinct lithospheric domains that closely correspond to established tectonic features of the WSB. For instance, Cluster 1 is associated with a stable, thick lithosphere in the central part of the basin, whereas Cluster 3 is indicative of rift-related zones characterized by thin crust and significant sedimentary accumulation. This methodology, implemented here for the first time for tectonic regionalization based on integrated lithospheric structure and thermal state, demonstrates its effectiveness by objectively capturing the multi-stage tectonic evolution of the WSB, including Hercynian accretion, Mesozoic rifting, and subsequent subsidence [*Artyushkov and Chekhovich*, 2023; *Latyshev et al.*, 2025; *Vyssotski et al.*, 2006].

Independent validation was provided by the spatial distribution of hydrocarbon reserves. The majority of major oil fields in the WSB are localized within Clusters 1 and 3, which are characterized by moderate to high heat flow and moderate to thick sedimentary cover. The correspondence between cluster locations and hydrocarbon accumulations supports the reliability of the clustering approach, despite the absence of oil reserve data in the clustering input.

The methodology developed in this study provides a robust foundation for further analyses of lithospheric structure and thermal regimes based on similarity metrics. In particular, the clustering results can inform machine learning applications aimed at predicting thermal states and heat flow in regions with limited observational data. Future research could expand this framework by integrating gravity and probably magnetic anomaly data, which would refine cluster interpretations in transitional or patchy zones (e.g., inclusions of Cluster 6 within Cluster 2; Figure 5). Gravity anomalies, derived from satellite missions like GRACE, can map crustal density variations and isostatic adjustments, clarifying tectonic boundaries obscured by sedimentary cover [*Braitenberg and Ebbing*, 2009; *Kaban et al.*, 2016]. Magnetic data could highlight basement heterogeneities, such as ancient sutures or magmatic features from Paleozoic accretion and Triassic tectonic and igneous activity, improving domain delineation [*Ivanov*, 2007; *Saunders et al.*, 2005]. This enhancement could also extend the approach to a global context.

Further refinement of cluster interpretations may be achieved by incorporating additional geological and geophysical constraints. Moreover, applying supervised machine learning techniques, such as random forests, to clustered data could facilitate predictive modeling of heat flow, with cross-validation used to assess model accuracy.

Acknowledgments. This research was funded by the Russian Science Foundation (project No. 21-77-30010-P). We thank the two reviewers for their constructive comments and suggestions, which significantly improved the quality of this manuscript.

References

Artemieva I. M. Global 1° × 1° thermal model TC1 for the continental lithosphere: Implications for lithosphere secular evolution // Tectonophysics. — 2006. — Vol. 416, no. 1–4. — P. 245–277. — https://doi.org/10.1016/j.tecto.2005.11.022

Artemieva I. M. and Mooney W. D. Thermal thickness and evolution of Precambrian lithosphere: A global study // Journal of Geophysical Research: Solid Earth. — 2001. — Vol. 106, B8. — P. 16387–16414. — https://doi.org/10.1029/2000jb900439

Artyushkov E. V. and Chekhovich P. A. The Origin of the West Siberian Sedimentary Basin without Strong Crustal Stretching: An Analysis of Superdeep Drilling Data // Doklady Earth Sciences. — 2023. — Vol. 512, no. 2. — P. 1006–1013. — https://doi.org/10.1134/s1028334x23601517

Braitenberg C. and Ebbing J. New insights into the basement structure of the West Siberian Basin from forward and inverse modeling of GRACE satellite gravity data // Journal of Geophysical Research: Solid Earth. — 2009. — Vol. 114, B6. — https://doi.org/10.1029/2008jb005799

Breiman L. Random Forests // Machine Learning. — 2001. — Vol. 45, no. 1. — P. 5–32. — https://doi.org/10.1023/a:1010933404324

Brown D., Carbonell R., Kukkonen I., et al. Composition of the Uralide crust from seismic velocity (V p , V s), heat flow, gravity, and magnetic data // Earth and Planetary Science Letters. — 2003. — Vol. 210, no. 1/2. — P. 333–349. — https://doi.org/10.1016/s0012-821x(03)00143-2

Burgess S. D. and Black B. A. The Anatomy and Lethality of the Siberian Traps Large Igneous Province // Annual Review of Earth and Planetary Sciences. — 2025. — Vol. 53, no. 1. — P. 567–594. — https://doi.org/10.1146/annurev-earth-040722-105544

Calinski T. and Harabasz J. A dendrite method for cluster analysis // Communications in Statistics - Theory and Methods. — 1974. — Vol. 3, no. 1. — P. 1–27. — https://doi.org/10.1080/03610927408827101

Cherepanova Y., Artemieva I. M., Thybo H., et al. Crustal structure of the Siberian craton and the West Siberian basin: An appraisal of existing seismic data // Tectonophysics. — 2013. — Vol. 609. — P. 154–183. — https://doi.org/10.1016/j.tecto.2013.05.004

Clarke J. W. Genesis of the West Siberian Basin and its Petroleum Geology: A Recent Interpretation // International Geology Review. — 1994. — Vol. 36, no. 11. — P. 985–996. — https://doi.org/10.1080/00206819409465500

Dorofeeva R. and Duchkov A. Heat Flow variations in Siberia and neighboring regions: A new look // International Journal of Terrestrial Heat Flow and Applications. — 2022. — Vol. 5, no. 1. — P. 09–13. — https://doi.org/10.31214/ijthfa.v5i1.80

Duchkov A. D., Zheleznyak M. N., Ayunov D. E., et al. Geothermal Atlas of Siberia and the Far East. — 2012. — URL: http://sibgeotherm.ipgg.sbras.ru/ (visited on 01/27/2026).

Field A. Discovering statistics using IBM SPSS statistics. — 6th. — London : Sage Publications, 2024.

Fuchs S., Norden B., Neumann F., et al. Quality-assurance of heat-flow data: The new structure and evaluation scheme of the IHFC Global Heat Flow Database // Tectonophysics. — 2023. — Vol. 863. — P. 229976. — https://doi.org/10.1016/j.tecto.2023.229976

Gordienko I. V. Geodynamic evolution of late Baikalides and Paleozoids in the folded periphery of the Siberian craton // Russian Geology and Geophysics. — 2006. — Vol. 47, no. 1. — P. 51–67.

Guyon I. and Elisseeff A. An introduction to variable and feature selection // The Journal of Machine Learning Research. — 2003. — Vol. 3. — P. 1157–1182.

Haeger C., Petrunin A. G. and Kaban M. K. Geothermal Heat Flow and Thermal Structure of the Antarctic Lithosphere // Geochemistry, Geophysics, Geosystems. — 2022. — Vol. 23, no. 10. — https://doi.org/10.1029/2022gc010501

Hartigan J. A. and Wong M. A. Algorithm AS 136: A K-Means Clustering Algorithm // Applied Statistics. — 1979. — Vol. 28, no. 1. — P. 100–108. — https://doi.org/10.2307/2346830

Holt P. J., Hunen J. van and Allen M. B. Subsidence of the West Siberian Basin: Effects of a mantle plume impact // Geology. — 2012. — Vol. 40, no. 8. — P. 703–706. — https://doi.org/10.1130/g32885.1

Hubert L. and Arabie P. Comparing partitions // Journal of Classification. — 1985. — Vol. 2, no. 1. — P. 193–218. — https://doi.org/10.1007/bf01908075

Ivanov A. V. Evaluation of different models for the origin of the Siberian Traps // Special Paper 430: Plates, Plumes and Planetary Processes. — Boulder, Colorado : Geological Society of America, 2007. — P. 669–691. — https://doi.org/10.1130/2007.2430(31)

Jolliffe I. T. and Cadima J. Principal component analysis: A review and recent developments // Philosophical Transactions of the Royal Society A: Mathematical, Physical and Engineering Sciences. — 2016. — Vol. 374, no. 2065. — P. 20150202. — https://doi.org/10.1098/rsta.2015.0202

Kaban M. K., Stolk W., Tesauro M., et al. 3D density model of the upper mantle of Asia based on inversion of gravity and seismic tomography data // Geochemistry, Geophysics, Geosystems. — 2016. — Vol. 17, no. 11. — P. 4457–4477. — https://doi.org/10.1002/2016gc006458

Khafizov S., Syngaevsky P. and Dolson J. C. The West Siberian Super Basin: The largest and most prolific hydrocarbon basin in the world // AAPG Bulletin. — 2022. — Vol. 106, no. 3. — P. 517–572. — https://doi.org/10.1306/11192121086

Koller D. and Sahami M. Toward optimal feature selection // ICML'96: Proceedings of the Thirteenth International Conference on International Conference on Machine Learning. — San Francisco : Morgan Kaufmann, 1996. — P. 284–292.

Laske G., Masters G., Ma Z., et al. Update on CRUST1.0 - A 1-degree global model of Earth's crust // Geophysical Research Abstracts. — 2013. — Vol. 15. — EGU2013–2658.

Latyshev A., Panchenko I., Smirnova M., et al. The Permian-Triassic volcanic activity in the West Siberian basin: A buried silicic LIP coeval to the Siberian Traps // Gondwana Research. — 2025. — Vol. 141. — P. 246–264. — https://doi.org/10.1016/j.gr.2025.02.019

Mirkin B. Choosing the number of clusters // WIREs Data Mining and Knowledge Discovery. — 2011. — Vol. 1, no. 3. — P. 252–260. — https://doi.org/10.1002/widm.15

Mooney W. D., Barrera-Lopez C., Suárez M. G., et al. Earth Crustal Model 1 (ECM1): A 1° × 1° Global Seismic and Density Model // Earth-Science Reviews. — 2023. — Vol. 243. — P. 104493. — https://doi.org/10.1016/j.earscirev.2023.104493

Murphy B. S. PyKrige: Development of a kriging toolkit for Python // AGU Fall Meeting Abstracts. Vol. 2014. — 2014. — H51K–0753.

Neumann F., Norden B., Balkan-Pazvantoğlu E., et al. The 2024 Release of the Global Heat Flow Database (GHFDB): Quality Assessment, Metadata Standards, and a Century of Geothermal Data // Earth System Science Data Discussions. — 2025. — P. 1–48. — https://doi.org/10.5194/essd-2025-341

Nikolaev V. A. Methodology of geodynamic zoning based on factor and cluster analysis (on the example of the East European Platform, Pannonian Basin and Northern Eurasia as a whole) : PhD thesis / Nikolaev V. A. — Moscow : Moscow State University, 2005. — 317 p. — (In Russian).

Pasyanos M. E., Masters T. G., Laske G., et al. LITHO1.0: An updated crust and lithospheric model of the Earth // Journal of Geophysical Research: Solid Earth. — 2014. — Vol. 119, no. 3. — P. 2153–2173. — https://doi.org/10.1002/2013jb010626

Pavlov Yu. A. On the Problem of Rift Structures in the West-Siberian Plate Basement // Geotektonica. — 1995. — No. 3. — P. 23–35. — (In Russian).

Pedregosa F., Varoquaux G., Gramfort A., et al. Scikit-learn: Machine Learning in Python // arXiv. — 2012. — P. 2825–2830. — https://doi.org/10.48550/ARXIV.1201.0490

Peterson J. A. and Clarke J. W. Geology and Hydrocarbon Habitat of the West Siberian Basin. — American Association of Petroleum Geologists, 1991. — https://doi.org/10.1306/st32544

Priestley K. and McKenzie D. The relationship between shear wave velocity, temperature, attenuation and viscosity in the shallow part of the mantle // Earth and Planetary Science Letters. — 2013. — Vol. 381. — P. 78–91. — https://doi.org/10.1016/j.epsl.2013.08.022

Puchkov V. N. Structure and geodynamics of the Uralian orogen // Geological Society, London, Special Publications. — 1997. — Vol. 121, no. 1. — P. 201–236. — https://doi.org/10.1144/gsl.sp.1997.121.01.09

Reichow M. K., Pringle M. S., Al'Mukhamedov A. I., et al. The timing and extent of the eruption of the Siberian Traps large igneous province: Implications for the end-Permian environmental crisis // Earth and Planetary Science Letters. — 2009. — Vol. 277, no. 1/2. — P. 9–20. — https://doi.org/10.1016/j.epsl.2008.09.030

Rousseeuw P. J. Silhouettes: A graphical aid to the interpretation and validation of cluster analysis // Journal of Computational and Applied Mathematics. — 1987. — Vol. 20. — P. 53–65. — https://doi.org/10.1016/0377-0427(87)90125-7

Saunders A. D., England R. W., Reichow M. K., et al. A mantle plume origin for the Siberian traps: uplift and extension in the West Siberian Basin, Russia // Lithos. — 2005. — Vol. 79, no. 3/4. — P. 407–424. — https://doi.org/10.1016/j.lithos.2004.09.010

Schaeffer A. J. and Lebedev S. Global shear speed structure of the upper mantle and transition zone // Geophysical Journal International. — 2013. — Vol. 194, no. 1. — P. 417–449. — https://doi.org/10.1093/gji/ggt095

Şengör A. M. C., Natal'in B. A. and Burtman V. S. Evolution of the Altaid tectonic collage and Palaeozoic crustal growth in Eurasia // Nature. — 1993. — Vol. 364, no. 6435. — P. 299–307. — https://doi.org/10.1038/364299a0

Shapiro N. M. and Ritzwoller M. H. Inferring surface heat flux distributions guided by a global seismic model: particular application to Antarctica // Earth and Planetary Science Letters. — 2004. — Vol. 223, no. 1/2. — P. 213–224. — https://doi.org/10.1016/j.epsl.2004.04.011

Sokolov S. Yu. and Mazarovich A. O. Cluster analysis of geological and geophysical parameters of the Arctic region as the base for geodynamic interpretation // Geodynamics & Tectonophysics. — 2016. — Vol. 7, no. 1. — P. 59–83. — https://doi.org/10.5800/gt-2016-7-1-0197

Stein M. L. Interpolation of spatial data: Some theory for Kriging. — New York : Springer, 1999. — https://doi.org/10.1007/978-1-4612-1494-6

Thrastarson S., Herwaarden D. P. van, Noe S., et al. REVEAL: A Global Full-Waveform Inversion Model // Bulletin of the Seismological Society of America. — 2024. — Vol. 114, no. 3. — P. 1392–1406. — https://doi.org/10.1785/0120230273

Tozer B., Sandwell D. T., Smith W. H. F., et al. Global Bathymetry and Topography at 15 Arc Sec: SRTM15+ // Earth and Space Science. — 2019. — Vol. 6, no. 10. — P. 1847–1864. — https://doi.org/10.1029/2019ea000658

Ulmishek G. F. Petroleum geology and resources of the West Siberian Basin, Russia // U.S. Geological Survey Bulletin. — 2003.

Verma M. K. and Ulmishek G. F. Reserve Growth in Oil Fields of West Siberian Basin, Russia // Natural Resources Research. — 2003. — Vol. 12, no. 2. — P. 105–119. — https://doi.org/10.1023/a:1024210711618

Vetrov E. V., Grave J. De, Vetrova N. I., et al. Tectonic Evolution of the SE West Siberian Basin (Russia): Evidence from Apatite Fission Track Thermochronology of Its Exposed Crystalline Basement // Minerals. — 2021. — Vol. 11, no. 6. — P. 604. — https://doi.org/10.3390/min11060604

Vibe Yu., Bunge H. P. and Clark S. R. Anomalous subsidence history of the West Siberian Basin as an indicator for episodes of mantle induced dynamic topography // Gondwana Research. — 2018. — Vol. 53. — P. 99–109. — https://doi.org/10.1016/j.gr.2017.03.011

Vyssotski A. V., Vyssotski V. N. and Nezhdanov A. A. Evolution of the West Siberian Basin // Marine and Petroleum Geology. — 2006. — Vol. 23, no. 1. — P. 93–126. — https://doi.org/10.1016/j.marpetgeo.2005.03.002

Witten D. M. and Tibshirani R. A Framework for Feature Selection in Clustering // Journal of the American Statistical Association. — 2010. — Vol. 105, no. 490. — P. 713–726. — https://doi.org/10.1198/jasa.2010.tm09415